Infection Dynamics of SARS-CoV-2 in Mucus Layer of the Human Nasal Cavity − Nasopharynx

Hanyu Li[1*], *Kazuki* Kuga[2], and *Kazuhide* Ito[2]

[1]Interdisciplinary Graduate School of Engineering Sciences, Kyushu University, Japan
[2]Faculty of Engineering Sciences, Kyushu University, Japan

Abstract. Severe acute respiratory syndrome coronavirus 2 (SARS-CoV-2) has led to the worldwide spread of coronavirus disease-2019 (COVID-19) since its emergence in 2019. Virus replication and infection dynamics after its deposition on the respiratory tissues require detailed studies for infection control. This study focused primarily on SARS-CoV-2 dynamics in the mucus layer of the nasal cavity and nasopharynx, based on coupled computational fluid-particle dynamics (CFPD) and host-cell dynamics (HCD) analyses. Considering the mucus milieu, we coupled the target-cell limited model with the convection-diffusion term to develop an improved HCD model. The infection dynamics in the mucus layer were predicted by a combination of the mucus flow field, droplet deposition distribution, and HCD. The effect of infection rate, β, was investigated as the main parameter of HCD. The results showed that the time series of SARS-CoV-2 concentration distribution in the mucus layer strongly depended on diffusion, convection, and virus production. β affected the viral load peak, its arrival time, and duration. Although the SARS-CoV-2 dynamics in the mucus layer obtained in this study have not been verified by appropriate clinical data, it can serve as a preliminary study on the virus transmission mode in the upper respiratory tract.

1 Introduction

The COVID-19 pandemic caused by a novel SARS-CoV-2 coronavirus has plagued global citizens with a heavy human toll for over two years. SARS-CoV-2 and its variants can cause high upper respiratory tract viral loads through airborne transmission, which requires further study [1][2]. However, mucus flow towards the pharynx by mucociliary motion is an indispensable biological defense for airborne respiratory infections. Here, we combined computational fluid and particle dynamics (CFPD) and host-cell dynamics (HCD) with a 3D-shell human airway model to predict the infection dynamics of SARS-CoV-2 in the mucus layer of the human nasal cavity and nasopharynx.

2 Methods

A 3D-shell model with a mucus layer of 15 μm thickness was established based on a volunteer's nasal cavity and nasopharynx, as shown in Fig. 1.

A worst-case scenario was assumed, in which a healthy person inhaled 10,000 droplets coughed from an infected person in close conversation. Since over 70% of droplets were less than 10 μm in diameter based on previous studies [3][4], we selected five particle sizes (1, 2.5, 5, 7.5, and 10 μm) as representatives for the particle distribution analysis, in accordance with a previous study [5].

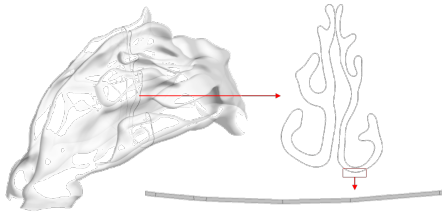

Fig. 1. 3D-shell model of the nasal cavity and nasopharynx.

In addition, we coupled the target cell-limited model [6] with the convection-diffusion of mucociliary motion to predict the viral load distributions, as follows:

$$\frac{\partial V}{\partial t} + U_i \frac{\partial V}{\partial x_i} = D_m \frac{\partial^2 V}{\partial {x_i}^2} + \frac{p'}{V_{mucus}} I - cV, \quad (1)$$

$$\frac{dT}{dt} = -\beta TV, \quad (2)$$

$$\frac{dI}{dt} = \beta TV - \delta I; \quad (3)$$

where V, T, and I represent the viral load, the number of target cells, and the number of infected cells, respectively. The equations also included velocity (U = 10 mm/min), virus diffusion coefficient (D_m = 2.91×10^{-12} m^2/s), virus production rate (p' = 0.74 copies/day/cell), mucus volume (V_{mucus} = 0.32 mL), virus clearance rate (c = 2.4/d), infection rate (β = 4.71×10^{-8} mL/copies/day) and infected cell clearance rate (δ = 1.07/d) [6]. $T(0)$ was assumed to be 8.46 × 10^8 cells. Fig. 2 depicts four focal spots of the droplets chosen as the sources of virus spread in this analysis. The initial viral counts (copies)

* Corresponding author: li.hanyu@kyudai.jp

in the right/left agger nasi, left inferior nasal concha, and nasopharynx were 2.71×10^{-4}, 1.17×10^{-4}, 2.21×10^{-5}, and 2.95×10^{-5}, respectively. Two cases were simulated: *Case 1* with virus diffusion and *Case 2* with virus convection (by mucus flow) and diffusion.

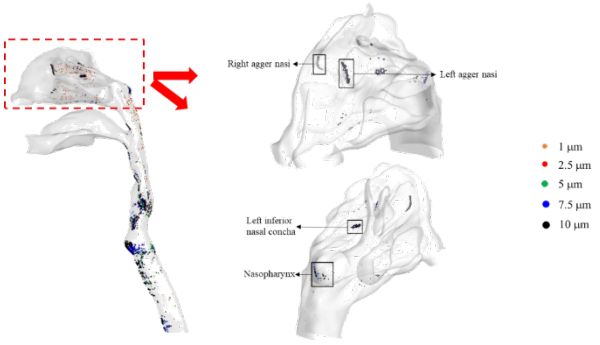

Fig. 2. Four focal spots of the droplets chosen as the sources of virus spread.

The parameters of the HCD model are crucial to fit the prediction results to the limited clinical data at present. This study mainly focused on the infection rate, β, of the target cells. Based on current studies, seven different β values, shown in Table 1, were substituted into the equations to assess their effects on SARS-CoV-2 infection dynamics.

Table 1. Different β (mL/copies/d) values observed in cases.

No.	β	No.	β
0	4.71×10^{-8}	**4**	1×10^{-5}
1	1×10^{-2}	**5**	1×10^{-6}
2	1×10^{-3}	**6**	1×10^{-7}
3	1×10^{-4}	**7**	1×10^{-8}

3 Results

As shown in Fig. 3, the trends of the average and maximum viral loads within 50 days in the two cases were determined.

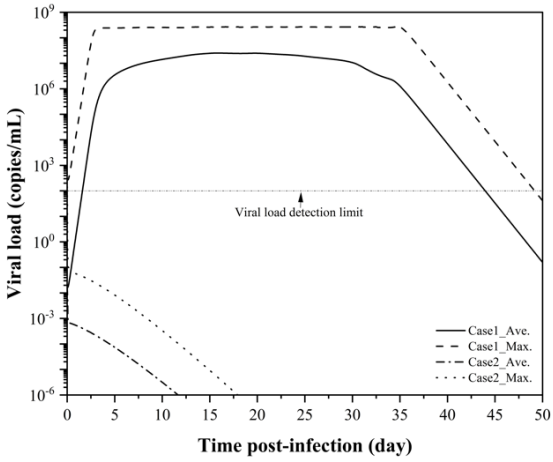

Fig. 3. The viral load of two cases over a period of 50 days.

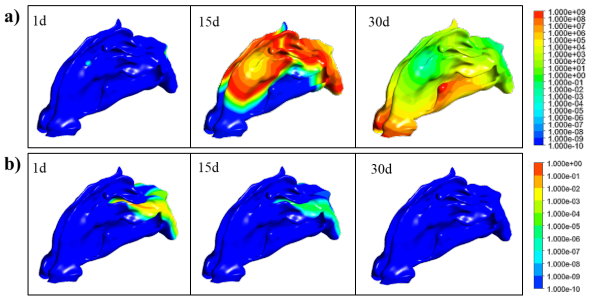

Fig. 4. Time series of SARS-CoV-2 replication in the mucus layer of the upper airway in a) *Case 1* and b) *Case 2*.

For *Case 1*, the viral load could be detected 2 days after infection, and it peaked at around day 15, where it remained for about 6 days and then declined below the detection limit on day 44. For *Case 2*, the viral load was minuscule and remained below detection because of the high convective velocity of mucus flow compared to the virus diffusive rate and infection rate. A visualization of SARS-CoV-2 infection dynamics for both cases is shown in Fig. 4.

However, these results are not consistent with the current clinical data. Therefore, β may be one of the main parameters in the HCD model.

Fig. 5 a) describes the viral load calculated directly by the target cell-limited model (without convection and diffusion term in Equation (1)), while Fig. 5 b) and c) show the viral load results in *Case 1* and *Case 2*, respectively, compared with the clinical data of 9 patients (a–i) [1]. Eight cases with different β values, including the original $\beta0$, were simulated simultaneously. The results from all three methods showed that β had a significant impact on the peak time. Moreover, the last two indicated that β affected the peak value and duration more for the cases that combined HCD and CFPD within the mucus milieu. Undoubtedly, the consequences from the direct calculation of the HCD model with $\beta0$ were consistent with the trend in clinical value.

Nevertheless, the results of the two cases in this study, coupled with the mucus environment, were significantly different. *Case 1* (Fig. 5b) revealed that larger β values corresponded to faster peak times and shorter durations. Furthermore, the trend line of $\beta4$ showed more consistency with previous clinical data of sputum. Likewise, *Case 2* (Fig. 5c) showed similar general values, whereas the contradiction among the infection rate, diffusive rate, and mucus flow velocity led to entirely different prediction curves. The findings peaked slightly at approximately one day after infection and decayed quickly. Notably, almost all curves had slight bimodal characteristics, and $\beta5$ was the optimal value considering this. Although their peak values did not reach the clinical peak values mentioned in this study, other studies, such as Fatehi et al. (2021) [7], have mentioned peak values in the range of 10^4–10^7 copies/mL, which is an important consideration for future studies.

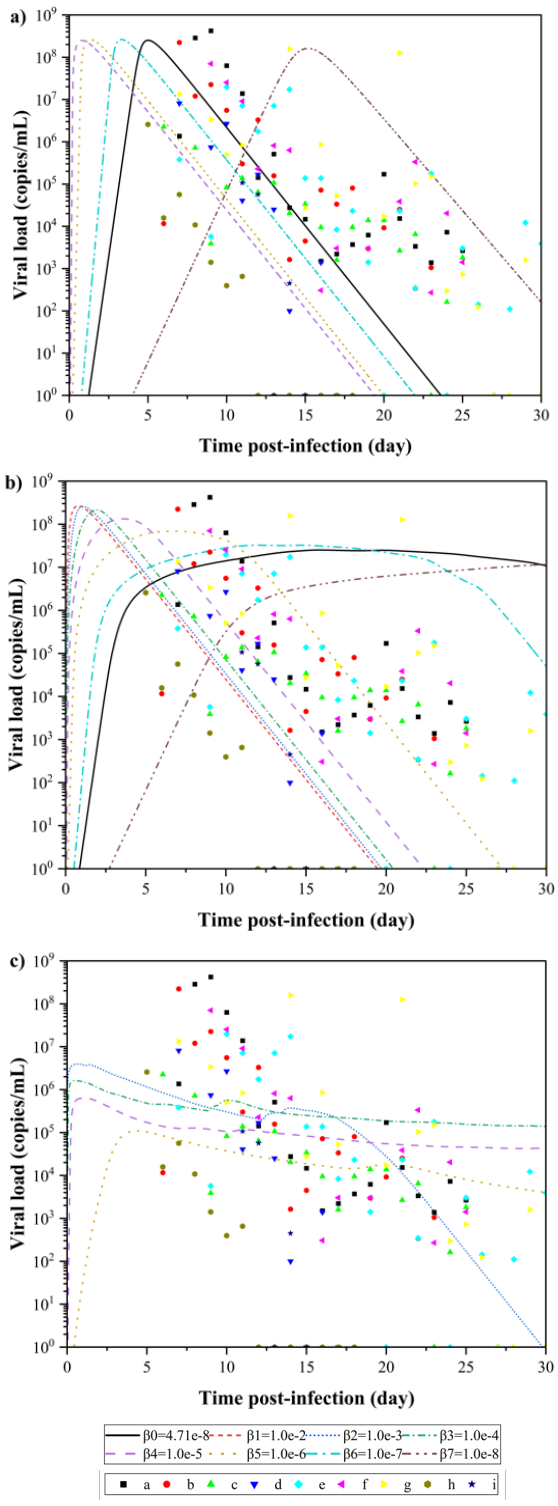

Fig. 5. Effects of different β values on the viral load.

4 Discussions

This study presented several limitations. Owing to ethical issues, it was not possible to conduct a corresponding verification experiment, which makes it difficult to verify the simulation results. Hence, we would need to collect as much data after infection or symptom onset as possible for comparative analysis.

In addition, the target cell-limited model used in this study was simplistic and did not consider any immune responses. Further, β is not a constant and may vary dynamically with viral load. Additionally, with the particle tracking analysis in this study being based on a steady CFPD calculation, a transient calculation should be attempted where different distributions may occur.

5 Conclusions

In this study, CFPD and HCD were combined with the nasal mucus environment to simulate and predict SARS-CoV-2 infection dynamics and the effects of infection rate on the results. In the case of the droplet deposition distribution in the upper respiratory tract calculated by a steady CFPD calculation, when considering the dynamics of SARS-CoV-2 in the mucus environment, the results of *Case 1* and *Case 2* showed that the peak time, peak value, and duration changed correspondingly. The results obtained using the original parameter values were entirely different from the existing clinical data. As an important parameter of HCD, the infection rate was adjusted in different cases, and the findings showed that β had a significant influence on the three different calculation methods. Using the target cell-limited model directly, the viral load value obtained using $\beta 0 = 4.71\times10^{-8}$ mL/copies/d was consistent with the clinical data with relatively consistent changes. In *Case 1*, the viral load at the magnitude of $\beta 4$ was 1×10^{-5} mL/copies/d, which was more consistent with the trend of the clinical data. For *Case 2*, there was a slight bimodal phenomenon, which is worth studying in combination with immune response. Although these simulated results have not been validated experimentally, they will contribute to a preliminary understanding of SARS-COV-2 infection dynamics in the mucus layer of the nasal cavity and nasopharynx. Thus, the study will greatly help develop intranasal drugs to prevent and treat COVID-19.

References

1. R. Wölfel *et al.*, *Nature*, vol. **581**, no. 7809, pp. 465–469 (2020)
2. R. Ke, C. Zitzmann, D. D. Ho, R. M. Ribeiro, and A. S. Perelson, *Proc. Natl. Acad. Sci. U. S. A.*, vol. **118**, no. 49, e2111477118 (2021)
3. J. P. Duguid, *J. Hyg. (Lond).*, vol. **44**, no. 6, pp. 471–479 (1946)
4. S. Yang, G. W. Lee, C. M. Chen, C. C. Wu, and K. P. Yu, *J. Aerosol Med.,* vol. **20**, no. 4, pp. 484–494 (2007)
5. N. L. Phuong, N. D. Khoa, and K. Ito, *Indoor Built Environ.*, vol. **29**, no. 6, pp. 793–809 (2020)
6. E. A. Hernandez-Vargas and J. X. Velasco-Hernandez, *Annu Rev Control*, vol. **50**, no. September, pp. 448–456 (2020)
7. F. Fatehi, R. J. Bingham, E. C. Dykeman, P. G. Stockley, and R. Twarock, *R. Soc. Open Sci.*, vol. **8**, no. 8, 210082 (2021)